Published in final edited form as:
Dev Neurobiol. 2013 December ; 73(12): . doi:10.1002/dneu.22119.

Neural stem cell apoptosis after low methylmercury (MeHg) exposures in postnatal hippocampus produce persistent cell loss and adolescent memory deficits

Katie Sokolowski[1], **Maryann Poku**[2], **Kelsey Robinson**[3], **Elizabeth McCandlish**[4,5], **Brian Buckley**[4,5], and **Emanuel DiCicco-Bloom**[1,2,4,5,6]

[1]Joint Graduate Program in Toxicology, GSBS, Rutgers University/ UMDNJ-Robert Wood Johnson Medical School, Piscataway, New Jersey

[2]Neuroscience and Cell Biology, UMDNJ-Robert Wood Johnson Medical School, Piscataway, New Jersey

[3]Rutgers University, New Brunswick, New Jersey

[4]UMDNJ Center for Environmental Exposures and Disease, Piscataway, New Jersey

[5]Environmental and Occupational Health Sciences Institute, Rutgers University, Piscataway, New Jersey

[6]Department of Pediatrics, UMDNJ-Robert Wood Johnson, Medical School, New Brunswick, New Jersey

Abstract

The developing brain is particularly sensitive to exposures to environmental contaminants. In contrast to the adult, the developing brain contains large numbers of dividing neuronal precursors, suggesting that they may be vulnerable targets. The postnatal day 7 (P7) rat hippocampus has populations of both mature neurons in the CA1-3 region as well as neural stem cells (NSC) in the dentate gyrus (DG) hilus, that actively produce new neurons that migrate to the granule cell layer (GCL). Using this well-characterized NSC population, we examined the impact of low levels of MeHg on proliferation, neurogenesis, and subsequent adolescent learning and memory behavior. Assessing a range of exposures, we found that a single subcutaneous injection of 0.6μg/g MeHg in P7 rats induced caspase activation in proliferating NSC of the hilus and GCL. This acute NSC death had lasting impact on the DG at P21, reducing cell numbers in the hilus by 22% and the GCL by 27%, as well as reductions in neural precursor proliferation by 25%. In contrast, non-proliferative CA1-3 pyramidal neuron cell number was unchanged. Furthermore, animals exposed to P7 MeHg exhibited an adolescent spatial memory deficit as assessed by Morris water maze. These results suggest that environmentally relevant levels of MeHg exposure may decrease NSC populations and, despite ongoing neurogenesis, the brain may not restore the hippocampal cell deficits, which may contribute to hippocampal-dependent memory deficits during adolescence.

Keywords

Neural stem cell; apoptosis; methylmercury; hippocampus; development

The authors declare no conflicts of interest.

Introduction

Initially, MeHg was found to have devastating effects on the developing brain during two poisoning events in Japan and Iraq, where apparently unaffected mothers delivered severely injured infants (Amin-Zaki et al., 1974, Harada, 1978). Although catastrophic poisonings rarely occur today, people are chronically exposed to low levels of MeHg through diet and may accumulate ~300 ppb of mercury (Hg) in their hippocampus (Lapham et al. 1995). The Seychelle and Faroe Islanders are two well-studied human populations who subsist on a fish diet, which contains low levels of MeHg. Studies in the Seychelles have found correlations of Hg exposure to memory functions (Grandjean et al., 1997), while studies of the Faroe Islanders show none (Myers et al., 2003, Davidson et al., 2006). The lack of memory deficits seen in the Faroe Island studies may, in part, be due to the nutritious polyunsaturated fatty acids (PUFA) found in cold water seafoods of the Faroe Islands (Strain et al., 2012). This raises the concern that the detrimental effects of MeHg on memory in human populations may be masked by the beneficial effect of PUFA. Memory formation is a major function of the hippocampus in humans and rodents (Morris et al., 1982; Eichenbaum et al., 2007). Animal studies indicate that the hippocampus is a target of MeHg with detrimental effects on learning and memory (Falluel-Morel et al., 2007, Onishchenko et al., 2007). By using animal models, we may define a threshold level of MeHg exposure that both reflects relevant Hg levels in the target tissue (~300 ppb) and affects hippocampal development and later cognition. This study potentially provides insight into the variability in human sensitivity to mercury exposure.

Mothers who gave birth to affected infants were exposed to MeHg during their third trimester (Amini-Zaki et al., 1974), a stage of hippocampal development that is equivalent to the first postnatal week in rodents (Rice and Barone 2000). Studies modeling *in utero* human exposures by using postnatal rat pups, show that MeHg induces mitotic arrest and caspase-dependent apoptosis (Rodier et al., 1984, Burke et al., 2006, Falluel-Morel et al., 2007, Sokolowski et al., 2011), suggesting that proliferative cell populations may be especially vulnerable to MeHg-induced cell death. Here, in similar models of MeHg exposure, we use single cell analysis techniques to identify deficits in specific populations of cells. Proliferative cells in the hippocampus express stage-specific markers as they progress from Sox2- and nestin-expressing multipotent neural stem cells (NSC), to neural progenitor cells, to immature and then mature neurons (Kempermann et al., 2004). Using select markers, previous studies indicate that NSC in culture are particularly sensitive to MeHg toxicity (Tamm et al., 2006, Xu et al., 2010). However, whether NSC are vulnerable to MeHg in the developing hippocampus with behavioral consequences remains undefined. We hypothesize that MeHg, at threshold levels approximating human exposures, will target NSC in the developing hippocampus and lead to later cellular and behavioral deficits. If our hypothesis is correct, this will be the first study to identify NSC as a target for MeHg in an *in vivo* model of the developing hippocampus.

Neurogenesis within the hippocampus occurs at different developmental periods in two primary neuronal populations: pyramidal neurons of Ammon's Horn (CA1-3) are generated prenatally, while the majority of dentate gyrus (DG) granule cells are generated postnatally in the hilus and migrate out to form the GCL before compaction of the subgranule zone (SGZ) (Bayer and Altman, 1975, Schlessinger et al., 1975, Altman and Bayer, 1990). Thus we may expect that a postnatal MeHg exposure, should it target NSC, may induce apoptosis in DG; while CA1-3 cells, generated prenatally, would be unaffected. Previous studies using the same model have found 5μg/g MeHg to have specific effects on the DG with persistent cellular and profound learning deficits (Falluel-Morel et al., 2007). However, in this study we identify and use NSC as targets to define a ten-fold lower exposure threshold that elicits cellular and behavioral effects. Single cell analysis of NSC is a more precise measure of

biological damage that enabled the detection of the effects of MeHg at environmentally relevant levels, thereby providing a model that more faithfully represents human exposures. Such a model would be beneficial in predicting harmful effects in the human population. Therefore, we aimed to answer two major questions: After *in vivo* exposure to relevant levels of MeHg 1) are NSC in the hippocampus vulnerable and 2) does the adolescent hippocampus recover from the initial acute effects of MeHg?

Methods

Animals

Female Sprague–Dawley rats with litters of twelve 4-day-old (P4), cross-fostered, male pups were purchased from Hilltop Lab Animals (Philadelphia, PA, USA). To achieve 12 male pups / litter, cross-fostering of pups was instituted by Hilltop prior to our receiving the animals. They were housed in a temperature- and light-controlled animal care facility and given food and water *ad libitum*. At P7, rats from the same litter were injected subcutaneously (sc) with vehicle (phosphate-buffered saline, PBS) or MeHg (0.2μg/gbw - 5μg/gbw) in a 100 μL bolus, constituting a within-litter dosing design. Therefore, 12 pups from a single litter were divided into 2, 3, or 4 groups, resulting in 6, 4, or 3 pups / experimental group, respectively, in each experiment. One litter was used for a single experiment; each experiment was performed three to four separate times. Although maternal care is known to affect developmental neurogenesis, the presence of all experimental groups in each litter mitigates against a group bias. Further, effects within each pup may reflect variability in biological response and injection efficacy. Thus sample size (n) was based on the number of pups. Although environmental exposure may be modeled through gastric lavage, sc injection was selected to ensure equal exposures for quantitative kinetic studies (see Table 1). Furthermore, absorption of MeHg through the gut may vary depending on gut contents and the numbers and types of enzymes that may differ in developing animals. Each figure has specific sample size (n) in the figure legend. All animal procedures were approved by the Robert Wood Johnson Medical School Institutional Animal Care and Utilization Committee (IACUC) and conformed to NIH Guidelines for animal use.

Materials

Methylmercury chloride (CH_3HgCl) was purchased from Sigma (St Louis, MO, USA). A 1.5 mg/ml stock solution in 0.1M PBS was prepared by agitation immediately before use.

Inductively coupled plasma – mass spectrometry—P7 rat pups were administered a single sc injection of vehicle or MeHg (0.6μg/g or 5μg/g body weight). Animals were perfused with 0.9% NaCl to flush blood from tissues. Whole hippocampi were collected for analysis at 2h, 24h, P21 and P35. These time points were chosen for their relevance to our prior mechanistic studies (2h – 24h) (Sokolowski et al., 2011), and our current studies on cell characterization (24h), stereological measures (P21), and behavior (P35). Three animals / MeHg group / timepoint were used, while only three control animals from P7 were used, totaling 27 animals. Hippocampal tissues (>100mg wet weight) were placed into a conical tube. To each tube 0.25mL of concentrated nitric acid (EMD OmniTrace Ultra High Purity, VWR Scientific) was added and the samples were allowed to react during active sonication. They were subsequently digested using a MARSX microwave sample digester (CEM Corp., Mathews NC). Final concentrations were diluted to 5% acid using DI water (MilliQ Ultrapure De-ionized, Millipore Corp., Billerica, MA) for a total volume of 7mL. Internal standards and controls included: acid blank, acid spike, matrix blank and matrix spike. The acid blank had no tissue and no Hg added, while the acid spike had a known amount of Hg added. The matrix spike was an untreated piece of tissue with a known amount of Hg added. Samples were analyzed for Hg using an X5 (Thermo Electron, MA)

inductively coupled plasma mass spectrometer (ICP/MS). The m/z of 202 was used for quantitation, while m/z of 199, 200 and 201 were also observed as a QC measure.

BrdU—Either P8 (Figure 1) or P21 (Figure 6) animals were given a single intraperitoneal injection of 100μg/g bromodeoxyuridine (BrdU). Animals were perfused for tissue fixation as below at 3hrs after BrdU injection. This interval was chosen so that cells incorporating BrdU did not have enough time to complete S, G2 and M phases and undergo cell division (producing 2 cells), thus specifically labeling cells in S phase. Brains were then processed for immunohistochemistry.

Immunohistochemistry—Animals were perfused with 0.9% NaCl followed by 1% paraformaldehyde in 0.1 mol/L PBS. Brains were post-fixed in 1% paraformaldehyde in PBS for 2h at 4°C, cryoprotected in 30% sucrose in PBS for 3 days at 4°C. Brains were embedded in Tissue-Tek (Sakura, Tokyo, Japan), and stored at −80°C until they were sectioned. Coronal sections (12 μm) were obtained on a cryostat (Leica, Heidelberg, Germany). Sections were incubated serially in boiling 0.01 mol/L citrate buffer (3 × 30 min) or steamed at 95°C, followed by hydrogen peroxide (0.3% in methanol, 10 min), 5% normal serum in PBS for 1 h, and then primary antibody overnight at 4°C in 0.3% Triton X-100 and 1% normal serum in PBS. We used the following primary antibodies: rabbit monoclonal anti-cleaved-caspase-3 (1:200; Cell Signaling, Beverly, MA, USA), mouse monoclonal anti-nestin (1:500; Millipore, Temecula, CA, USA), mouse monoclonal anti-Sox2 (1:500; Sigma-Aldrich, St. Louis, MO, USA), and mouse monoclonal anti-BrdU (1:100; Becton-Dickinson, San Jose, CA, USA). For single antigen staining, biotinylated goat anti-rabbit or anti-mouse IgG (Vector Laboratories, Burlingame, CA, USA) was applied as secondary antibodies and avidin–biotin peroxidase complex (ABC kit; Vector Laboratories) served as amplification reagent. Diaminobenzidine served as chromogen to localize the peroxidase. Quantification of positive cells, observed with a Zeiss Axiophot microscope (Zeiss/Sony, Tokyo, Japan), on bilateral hippocampi was performed on 4 sections/animal, every 10^{th} section of the middle third of the hippocampus (between Bregma −1.34 to −2.54mm, a region that is most proliferative at this age (Wagner et al., 1999; Cheng et al., 2002)), in 6 to 12 animals/group, obtained from three separate experiments. The first cell layer of the SGZ was included in the GCL, while the other SGZ cells were counted as part of the hilus. All positive cells present in the selected sections and regions were counted. BrdU and caspase-3 were rare events, therefore any differences detected between control and treated groups would have a large impact on later total cell number (as detected with stereology). However, hundreds of immunoreactive cells were counted in each group to produce the results reported. For caspase-3 approximately 6 – 25 cells were counted in each animal, and 6 animals were used, totaling 36 – 150 cells per treatment group. For BrdU, approximately 30 - 60 cells were counted in each individual animal, and 9 animals were used in each group, totaling 270 - 540 cells counted per treatment group. For double fluorescent immuno-staining the secondary antibodies used were Alexa Goat anti-Rabbit 594 and Alexa Goat anti-Mouse 488 (Molecular Probes, Eugene, OR, USA). Sections were visualized on an Axiovert 200M microscope (Zeiss, Thornwood, NY, USA) coupled to an Apotome module. Z-stack images were created and merged to positively identify double-labeled neurons (Figures 3 and 4). Cells were counted blind to experimental group at high magnification (≥40× objective).

Unbiased stereology for total cell analysis—Cell number was estimated in the hippocampus 2 weeks after MeHg exposure by using a Bioquant computerized image analysis system (Nashville, TN, USA). Color video images were obtained with the camera-imaging systemBioquant NOVA Prime Version 6.90.10MSR (Bioquant Image Analysis Corporation) on a Zeiss Axiophot microscope (Zeiss/Sony, Tokyo, Japan). Outlines of the

brain regions were drawn at low magnification, and nuclei were counted under 63× objective in oil (630× magnification). Cells counted in the first cell layer of SGZ were included in the 'GCL', while the other SGZ cells were counted as part of the 'hilus'. The cell number for each region (*N*) was estimated by using the following algorithm: *N* = total number cells counted × reciprocal of section sampling fraction × reciprocal of area sampling fraction × reciprocal of thickness sampling fraction, where section sampling fraction = number section sampled/total number of sections; area sampling fraction = counting from area/grid square area; and thickness sampling fraction = optical dissector height/mean tissue thickness. Independent variance was determined by computing the percentage of variance (Var from Nugget (Var = Nug + Estimated variance from systematic random sampling) (Cheng et al., 2002, Falluel-Morel et al., 2007). At P21, assessing every 10^{th} section through the entire extent of the hippocampus, data were obtained from 12-15 sections per animal. Sections were 12 μm each and stained with toluidine blue, facilitating the visibility of individual cells. Quantification of cells observed on unilateral hippocampi was performed for 9 animals/group, obtained from three independent experiments.

Spatial learning on the Morris water maze—A circular pool (180 cm diameter × 75 cm high) was filled to a depth of 45 cm with black opaque water at 22°C. The hidden platform was constructed of plexiglass (14 × 14 cm), painted black, and submerged 1.5 cm below water level. The maze was located in a 4 × 4-m room, and extra maze cues included posters, a door, and a cage. The maze was divided in four virtual quadrants: north (N), south (S), east (E), and west (W). During the acquisition of place learning and the recovery test, the platform was in the same position (in the middle of quadrant E). During *acquisition*, there were four trials each day, and the intertrial interval was 1 min. Each animal was released from one of the quadrants S, N, or W facing the wall of the pool. The order of the release positions was varied systematically throughout the experiment as follows: day 1: S-W-N-S; day 2: N-W-S-W; day 3: W-N-S-N; day 4: N-S-N-W; day 5: W-S-N-S; day 6: S-N-W-N; and day 7: N-S-W-S. A trial ended when the rat climbed onto the platform. If a rat had not found the platform after 90 s, it was placed on the platform by the researcher. The rat was left on the platform for 30 s and then removed to its home cage under a heating lamp by the experimenter. *Memory tests* were performed 2 days and 2 weeks after the last training day, and rats were released from quadrants W and N, respectively (platform remained in quadrant E to prevent extinction across memory trials). *Motivation, motor and visual abilities* were monitored after the last recovery test by using a visible platform that protruded 2.5 cm above the surface of the water in quadrant S. Results were obtained from a total of 30 male animals from five separate cross-fostered litters per group. The litters were split between controls and treatment groups. The experiments were performed four separate times. No litter effect was found (ANOVA comparing 5 litters within the same group provided p values > 0.1). Specifically, the p values for the 2-day memory trial across control litters were 0.70, across MeHg treated litters was 0.64, 2-week memory trials across control litters were 0.50, and across MeHg treated litters was 0.38. Only memory trials were scrutinized for litter effects since this was where significant deficits were found (i.e. no learning deficits detected). It is reasonable to assume that if there is no litter effect during the memory trials, there is most likely no litter effect during learning / acquisition.

Statistical evaluation—One-way ANOVA followed by Tukey–Kramer multiple comparison test was used for analysis of experiments involving three groups or more. An unpaired *t*-test with Welch's correction was used for analysis of experiments involving two groups. A repeated measure ANOVA (Statview 5.0.1) and a Mixed Model Analysis (SAS/STAT 9.2 software) were used to analyze significance for the Morris water maze, with group (control and MeHg) as the "between subjects" factor, and day or interval as the "within subjects" factor. The four trials / day were averaged to obtain a single escape latency

for an acquisition day. Probabilities of less than 0.05 were regarded as statistically significant. Data were expressed as arithmetic means ± SEM for all experimental measurements.

Results

Total Hg concentration in hippocampus after P7 MeHg exposure

To establish an experimental model of environmentally relevant MeHg exposure, we first had to determine the kinetics of brain-metal exposure, and compare hippocampal Hg burden in our model to that of human populations. Our target concentration of mercury (Hg) in the hippocampus is 300 ppb, a concentration found in hippocampal tissues of humans subsisting on a fish diet (Lapham et al., 1995). Hg was detected in the hippocampus as early as 2h after a single injection of 5μg/g MeHg, reaching 499 ppb. Hg concentrations increased after both exposures, 0.6μg/g and 5μg/g, with peak values at 24h. At peak, the 0.6μg/g MeHg dose resulted in concentrations of Hg very close to the target range in the hippocampus (383 ± 66 ppb; Mean ± SEM), and similar in range to human tissue levels (Lapham et al., 1995). As expected, peak tissue concentrations after exposure to 5μg/g MeHg were much higher (1,963 ± 157 ppb). Subsequently, Hg concentrations decreased to control levels by P21 after 0.6μg/g MeHg exposures and by P35 after 5μg/g MeHg (Table 1). These observations indicate that the developing brain is readily accessible to Hg following peripheral exposure to MeHg, yet has effective mechanisms for clearance that reflect levels of exposure. The tissue burden of Hg after a single injection of 0.6μg/g MeHg is remarkably similar to human tissue levels. Most importantly, Hg is present in the hippocampus during the peak of neurogenesis and undetected at later time points; thus making this a useful model to study the effects of MeHg selectively on neural progenitors.

Defining a threshold exposure to MeHg with effects on hippocampal NSC

Recent studies in culture have determined that nestin+ NSC are particularly vulnerable to low levels of MeHg exposure compared to mature neurons (Tamm et al., 2006). While previous studies have shown a reduction in mitosis within the hippocampus after MeHg exposure (Burke et al., 2006; Falluel-Morel et al., 2007), hippocampal NSC have not been conclusively identified as targets of MeHg *in vivo*. MeHg exposure induced a decrease in BrdU+ cells in two regions of the DG: the granule cell layer (GCL), and the hilus. A greater than 40% reduction in mitotic cells was observed in both regions at 5μg/g MeHg exposure (Fig. 1), replicating previous studies that also found a profound adolescent learning deficit (Falluel-Morel et al., 2007). However, even a ten-fold lower level of MeHg exposure (0.6μg/g) also significantly reduced BrdU+ cells in the hilus by 32% and the GCL by 27%, (Fig. 1).

Once the threshold dose affecting mitosis was established to be 0.6μg/g MeHg, the sensitivity of a specific population of mitotic cells, hippocampal NSC, was defined using the NSC marker, Sox2, in the DG (Suh et al., 2007). MeHg exposure produced an almost 2-fold reduction in the number of Sox2+ cells at 24h, with a similar effect using 0.6μg/g (Fig. 2), suggesting that NSC are targets of MeHg.

Effects of acute MeHg exposure on NSC cell death

Our initial reports demonstrated that the MeHg-induced decrease in proliferation was secondary to increased caspase-dependent apoptosis (Falluel-Morel et al., 2007; Sokolowski et al., 2011), suggesting that enhanced apoptosis may contribute to the loss of the NSC population. To more directly examine the relationship of apoptosis to the NSC population, we double-labeled cells with activated caspase-3, a marker of apoptosis, and a NSC marker, nestin or Sox2. With increasing exposures, there were 2-4-fold increases in caspase-3+ cells

in the hilus at 24h after MeHg injection on P7 (Figs. 3 and 4), a result consistent with previous data on caspase activation and increased cell pyknosis (Sokolowski et al., 2011). Further, there was also a dose-dependent increase in double-labeled, nestin-expressing precursors exhibiting caspase-3 (Fig. 3). The majority of the total caspase-3+ cells co-expressed NSC marker nestin (double-labeled / total caspase-3). More importantly, the proportion of activated caspase-3+ cells co-labeling with nestin increased from 65% in controls to greater than 75% in the 0.6μg/g and 5μg/g MeHg exposed animals at 24h (Fig. 3), suggesting that the majority of the MeHg-induced increase in apoptosis occurred selectively in the NSC population.

To further examine this issue, another NSC marker, Sox2, that co-labels many cells that express nestin, was used in the same paradigm. As with nestin, double-immunostaining with caspase-3 and Sox2 also revealed an exposure-dependent increase in the number of double-labeled cells (Sox2+-caspase-3+) (Fig. 4). The four-fold increase in the absolute number of Sox2 expressing cells that co-label with caspase-3 suggests that cell death plays an important role in the major loss of Sox2+ cells following MeHg exposure (Fig. 2b). However, unlike nestin-caspase-3 double-labeled cells, the relative proportion of dying cells exhibiting caspase-3 did not differ among MeHg exposure groups, suggesting that different stem cell subpopulations exhibit distinct vulnerabilities. Together, these studies suggest that hippocampal NSC are vulnerable to neurotoxic effects of MeHg at low exposure levels *in vivo*.

Effects of P7 exposure to 0.6μg/g MeHg on the P21 DG proliferative cell population

Reductions in DG proliferation have residual effects on hippocampal-dependent learning and memory function (Rola et al., 2004; Leuner et al., 2006). We asked the question, does an acute decrease in BrdU+ cells and loss of Sox2+ precursors in the hippocampus after P7 MeHg exposure lead to a lasting decrease in neurogenesis and cell numbers at later ages? To examine this issue, P7 rat pups were injected once with 0.6μg/g MeHg or PBS and allowed to develop into prepubescent rats, age P21. At this age, the hippocampus has nearly completed development and neurogenesis begins to decline to levels equivalent to the adult (Bayer and Altman, 1975, Schlessinger et al., 1975, Altman and Bayer, 1990). At the time of MeHg exposure (P7), there are abundant proliferating NSCs from P3 to P10 localized to the hilus (termed the tertiary dentate matrix, Altman and Bayer, 1990). However, at the time of analysis (P21), NSCs diminish in number between P20 to P30 and precursors become confined to the SGZ. Because of this evolving hippocampal cytoarchitecture, we analyzed the P21 brains for total cell number using stereology in five regions including three layers of the DG: hilus, GCL, and molecular layer (ML) and two layers of Ammon's Horn: pyramidal cell layer (PCL) and stratum radiatum (SR) (Fig. 5a). MeHg injection at P7 produced a 22% decrease in total cells in the hilus and a 27% reduction in the GCL at P21 (Fig. 5b), two regions that were actively undergoing neurogenesis at the time of exposure. In contrast, in the CA1-3 neuron populations that were mature at the time of injection, neither the PCL nor SR exhibited any changes. These results complement earlier studies using a similar single-exposure paradigm with a ten-fold higher level (5μg/g) of MeHg (Falluel-Morel et al., 2007), demonstrating the regional specificity of cell loss even after an especially low exposure of MeHg.

The stereology data suggest that proliferating regions of the DG are most vulnerable to the lasting effects of an acute exposure and raise the possibility that there is a sustained decrease in the proliferative pool of progenitors. To determine whether the progenitor pool was affected, neurogenic activity was estimated by assessing acute BrdU incorporation in adolescent pups after perinatal MeHg exposure (Fig. 6). A major decrease was observed in the number of BrdU+ cells in the P21 hilus: there was a 33% decrease after 5μg/g and a 24%

reduction after 0.6μg/g MeHg (Fig. 6). With regard to the 0.6μg/g MeHg exposure on P7, the decrease in neurogenesis defined at P21 occurred after the the time that Hg had been cleared from the brain (Table 1), suggesting that the acute loss of NSC soon after MeHg accounted for the later reduction in the progenitor pool.

Hippocampal-dependent memory performance during adolescence after P7 exposure to 0.6μg/g MeHg

While many animal studies have defined the effects of chronic MeHg exposure on adult behaviors, few have studied adolescent behaviors and only one other study has considered the effects of postnatal MeHg on adolescent learning and memory. In our previous study, P7 rats that were exposed to 5μg/g MeHg exhibited profound learning and memory deficits in the Morris water maze at P35 (Falluel-Morel et al., 2007), the adolescent period of rat development (Rice and Barone, 2000). Here, we use the same adolescent learning paradigm with a ten-fold lower postnatal exposure level of MeHg. Given the acute loss of NSC at P8 (Fig. 2) and the decreases in neuronal cell numbers (Fig. 5) and neurogenesis at P21 (Fig. 6), we explored possible correlations to hippocampal-dependent learning and memory behaviors. Since the hippocampus contributes to spatial learning and memory, adolescent animals (P35) were assessed in the Morris water maze. Both groups of animals were able to acquire the task, however, on the final two days of acquisition (day 6 and 7), MeHg exposed animals had significantly longer escape latencies than their littermate controls (Fig. 7a). Subtle differences during the acquisition perioddo not suggest a learning deficit; however, it could suggest a possible learning ‘disadvantage’. The learning disadvantage was further supported by the two-day memory trial, in which MeHg exposed animals took significantly longer than controls to find the hidden platform (Fig. 7b). The two-week memory trial revealed a tendency towards the same deficit ($p=0.057$), although the escape latencies of both groups increased, rendering results insignificant (Fig. 7c). Animals were also run on the visible platform test to assess possible impairments in motivation, motility, and sensory systems as contributing factors; there were no differences in groups on this task (Fig. 7d).

Discussion

Our observations indicate that NSCs of the postnatal hippocampus are especially sensitive to MeHg, at exposure levels previously considered inconsequential. Using a brain Hg level designed to mimic human exposure, we found that the metal rapidly accessed the brain and was cleared over weeks in an exposure-dependent fashion. The presence of Hg in the hippocampus during postnatal neurogenesis elicited acute NSC apoptosis, with no detectable effect on the more mature pyramidal neurons generated prenatally. In turn, by acutely targeting DG stem cells, the numbers of granule neurons weeks later, when Hg was cleared, were significantly reduced. The deficit in postnatal DG neurogenesis was accompanied by a modest impairment in adolescent spatial memory. Many studies have investigated the effects of adult MeHg exposure on adult behaviors, yet the human data finding learning deficits were performed in exposed children and adolescents. This is the first study to our knowledge analyzing adolescent learning and memory after such a low level of postnatal MeHg exposure. Presented here are the remarkable findings of acute reductions of NSCs correlated with adolescent memory defects after a single P7 exposure to very low levels (0.6μg/g) of MeHg.

Animals experiencing chronic exposures to comparably low levels of MeHg (0.5μg/g/day) throughout gestation and the first week after birth have shown memory impairments (Onishchenko et al., 2007). Using the single exposure paradigm established by Rodier (Rodier et al., 1984), our previous work indicated that a single injection of 5μg/g MeHg at P7 produced profound juvenile spatial learning impairment and decreases in cell number in P21 hippocampus that correlated with acute caspase-dependent apoptosis (Falluel-Morel et

al., 2007). These past studies, performed on whole hippocampal tissue homogenates, found that 3-5μg/g MeHg were the lowest levels of exposure that elicited decreases in DNA synthesis and neuronal numbers (Burke et al., 2006, Falluel-Morel et al., 2007). Here, using single cell analysis techniques on tissue sections, we are able to perform quantification of both mature neurons and mitotic progenitors and demonstrate the exquisite sensitivity of the NSC to a ten-fold lower level of MeHg exposure, 0.6μg/g. Significantly, this level of MeHg is near equivalent to a single day's exposure in some chronic exposure paradigms designed to mimic the human situation (Newland and Reile, 1999, Newland et al., 2006, Onishchenko et al., 2007). Furthermore, our study demonstrates that this low exposure produces hippocampal Hg levels (383ppb) similar to Seychellois infants of about 300ppb (Lapham et al., 1995). This work provides a useful model to test the threshold at which toxic exposures may compromise proliferating cells of the developing brain.

Stem cells are targets of MeHg-induced apoptosis

The current literature suggests that MeHg inhibits DNA synthesis and cell mitosis, however, not selectively. At very high exposure levels, MeHg can cause neuropathology in regions not known to contain actively dividing NSC, such as the calcarine cortex and cerebellar granule cell layer (Chang et al., 1977, Choi, 1989, Burbacher et al., 1990). Yet at much lower levels, more recent literature indicates that cultured NSCs are more sensitive to MeHg (Burke et al., 2006, Tamm et al., 2006, Falluel-Morel et al., 2007, Stummann et al., 2009).

Here we determined whether the impact of MeHg observed in cultured NSCs could translate to effects *in vivo*, by observing the vulnerability of NSCs to low levels of MeHg in the developing rat hippocampus. Acute P7 exposure to MeHg (0.6μg/g, 24h) resulted in decreases in BrdU labeled (S-phase marker) and nestin- or Sox2-expressing (NSC markers) cells of the DG. Reductions in these two markers suggest that MeHg is affecting not only dividing cells but can specifically target NSCs. Previous studies have shown that BrdU+ cells do co-label with the cell death marker, caspase-3 (Falluel-Morel et al., 2007), suggesting that the cell loss could be from caspase-mediated cell death. The effects of MeHg occurred especially in the NSC, as reflected by very high proportions of caspase-3+ cells co-labeling with NSC markers including Sox2 (38%) and nestin (75%). Furthermore, as MeHg elicited increasing levels of caspase-3+ cells, even greater proportions of the cells co-expressed nestin. However, in contrast to nestin/caspase-3 double-labeling, there was no change in the ratio of Sox2/caspase-3 cells. It is unclear to what degree the nestin/caspase-3 population overlaps with the Sox2/caspase-3 population. It is known, however, that nestin and Sox2 may not always co-label the same cell compartment (Kempermann et al., 2004, Steiner et al., 2006), suggesting that they identify different stages of neuronal maturation. While there is mounting evidence that caspases are involved in cell differentiation (Kuranaga and Miura, 2007), we previously found that MeHg induced both activated caspase-3 in parallel with pyknotic nuclei (Sokolowski et al., 2011) and MeHg can induce caspase-mediated cell death in cerebellum and hippocampus (Lu et al., 2011, Sokolowski et al., 2011). Considering the current results in conjunction with published data in similar paradigms demonstrating apoptosis, it appears that MeHg is targeting NSCs for cell death. Since NSCs generate cells that later differentiate into mature neurons, losses in this progenitor population has the potential to disrupt the number of cells produced later in life, and that are available to participate in hippocampal-dependent learning and memory (Leuner et al. 2006).

It is interesting to note that following the single 0.6μg/g MeHg injection, Hg concentrations in the hippocampus, that reflected the tissue burden measured in human brain (Lapham et al., 1995), returned to control levels by P21 and perhaps earlier. Since Hg was detectable only during DG development, this model may be ideal to study region-specific effects

during sensitive time windows. Based on the kinetics of Hg presented here, later structural and behavioral changes observed two weeks after injection were a result of the early insult rather than due to continuous cell damage from the presence of Hg.

Acute reductions in stem cells correlate with differences in cell number and adolescent memory

If exposure to low levels of MeHg at P7 can lead to decreases in NSC populations in the hippocampus, then it is possible to have lasting deficits in mature neuronal cell numbers. Taking advantage of the fact that the hippocampus contains post-mitotic pyramidal neurons in CA1-3 and mitotic neuronal progenitors in the DG, the present model demonstrates decreases in P21 hilus and GCL cells only, but not regions of CA1-3. Thus cell loss was detected in proliferative regions alone and not those that underwent prenatal neurogenesis (CA1-3). These results suggest that the initial loss of progenitors at P7-8 contributes to the prepubescent loss of cells in the P21 DG. Stereological quantification of five regions of the hippocampus not only demonstrates a lasting effect, but also suggests that MeHg induces a decrease in cells restricted to the hilus and GCL, likely to include the NSCs or nascent neurons. Although cell number was assessed after development of the hippocampus, it is possible, due to ongoing neurogenesis, to have recovery in the adult brain as observed after trimethyltin exposure (Ogita et al., 2005). Furthermore, we cannot exclude the possibility that early MeHg exposure altered the ability of new cells to migrate into the GCL, an additional mechanism to reduce mature neuron numbers. This question could be addressed by pre-labeling precursors with BrdU, and then tracking their migration rates after MeHg exposure.

The effects of MeHg on hippocampal neurogenesis naturally led to questions regarding possible functional consequences. The role of hippocampal granule neurons in learning or memory have been shown in rodent models using toxicants other than MeHg, including trimethyltin, (Fiedorowicz et al., 2001, Halladay et al., 2006), gamma irradiation (Snyder et al., 2005, Winocur et al., 2006), cytosine arabinoside (AraC) (Li et al., 2008) and methylazoxymethanol (MAM) (Shors et al., 2002). Using low levels of MeHg exposure during development, chronic exposures produced learning impairments in adult rodent models (Onishchenko et al., 2007, Newland et al., 2008). However, human studies found MeHg-associated behavioral deficits in children and did not investigate effects on the adult (Grandjean et al., 1997). Therefore, to describe adolescent learning impairments in our acute model, animals treated with 0.6μg/g MeHg or PBS at P7 were trained on the water maze at P35 to assess hippocampal function. Both groups of animals learned, thus there was no clear learning deficit. However, MeHg exposed animals exhibited a significant decrease in memory performance. Although subtle, these results emphasize the impact of acute loss of progenitors on adolescent behavior. Such subtle injuries that may reduce system resilience may in conjunction with other life experiences set the stage for later life cognitive impairments. Further exploration with behavioral tasks specific to hippocampal or cortical function may help further define the behavioral deficit. Additionally, despite the strong correlative evidence of decreased cell number and neurogenesis with function, other areas of the brain or body may contribute to altered hippocampal neurogenesis and/or behavioral differences through hormonal imbalance, for example.

Taken together, this set of experiments has pointed to the possibility that NSC losses may be early indicators or predictors of adolescent behavioral disruptions. Since we detected brain Hg levels relevant to human tissues, this model provides evidence of a threshold dose that may cause an increased risk to neurodevelopment disorders.

Acknowledgments

The research was supported by the CounterACT Program, National Institutes Of Health Office of the Director, and the National Institute of Environmental Health Sciences, 1R21ES019762 (E.D.-B), and supported by UMDNJ Center for Environmental Exposures and Disease, P30ES005022. Katie Sokolowski was supported by a training fellowship, NIH ES007148 20 T31, and was a recipient of an individual fellowship from NINDS, 1F31NS062591-01A2. Maryann Poku was a recipient of the IGERT Award NSF DGE, 0801620 and an individual fellowship from NINDS, 1F31NS082015. We would like to thank Dr. Pamela Ohman-Strickland for her guidance with the statistics, Dr. Kenneth Reuhl for his constant support and guidance on all matters MeHg, Dr. Helene Sisti for guidance in design and interpretation of the behavioral tasks and Dr. Joshua Corbin for his valuable comments to drafts of the manuscript.

References

Altman J, Bayer SA. Prolonged sojourn of developing pyramidal cells in the intermediate zone of the hippocampus and their settling in the stratum pyramidale. J Comp Neurol. 1990; 301:343–364. [PubMed: 2262595]

Amin-Zaki L, Elhassani S, Majeed MA, Clarkson TW, Doherty RA, Greenwood M. Intra-uterine methylmercury poisoning in Iraq. Pediatrics. 1974; 54:587–595. [PubMed: 4480317]

Bayer SA, Altman J. The effects of X-irradiation on the postnatally-forming granule cell populations in the olfactory bulb, hippocampus, and cerebellum of the rat. Exp Neurol. 1975; 48:167–174. [PubMed: 1132466]

Burbacher TM, Rodier PM, Weiss B. Methylmercury developmental neurotoxicity: a comparison of effects in humans and animals. Neurotoxicol Teratol. 1990; 12:191–202. [PubMed: 2196419]

Burke K, Cheng Y, Li B, Petrov A, Joshi P, Berman RF, Reuhl KR, DiCicco-Bloom E. Methylmercury elicits rapid inhibition of cell proliferation in the developing brain and decreases cell cycle regulator, cyclin E. Neurotoxicology. 2006; 27:970–981. [PubMed: 17056119]

Chang LW, Reuhl KR, Lee GW. Degenerative changes in the developing nervous system as a result of in utero exposure to methylmercury. Environ Res. 1977; 14:414–423. [PubMed: 590231]

Cheng Y, Black IB, DiCicco-Bloom E. Hippocampal granule neuron production and population size are regulated by levels of bFGF. Eur J Neurosci. 2002; 15:3–12. [PubMed: 11860501]

Choi BH. The effects of methylmercury on the developing brain. Prog Neurobiol. 1989; 32:447–470. [PubMed: 2664880]

Davidson PW, Myers GJ, Cox C, Wilding GE, Shamlaye CF, Huang LS, Cernichiari E, Sloane-Reeves J, Palumbo D, Clarkson TW. Methylmercury and neurodevelopment: longitudinal analysis of the Seychelles child development cohort. Neurotoxicol Teratol. 2006; 28:529–535. [PubMed: 16904865]

Echenbaum H, Yonelinas AR, Ranganath C. The medial temporal lobe and recognition memory. Annu Rev Neurosci. 2007; 30:123–152. [PubMed: 17417939]

Falluel-Morel A, Sokolowski K, Sisti HM, Zhou X, Shors TJ, Dicicco-Bloom E. Developmental mercury exposure elicits acute hippocampal cell death, reductions in neurogenesis, and severe learning deficits during puberty. J Neurochem. 2007; 103:1968–1981. [PubMed: 17760861]

Fiedorowicz A, Figiel I, Kaminska B, Zaremba M, Wilk S, Oderfeld-Nowak B. Dentate granule neuron apoptosis and glia activation in murine hippocampus induced by trimethyltin exposure. Brain Res. 2001; 912:116–127. [PubMed: 11532427]

Grandjean P, Weihe P, White RF, Debes F, Araki S, Yokoyama K, Murata K, Sorensen N, Dahl R, Jorgensen PJ. Cognitive deficit in 7-year-old children with prenatal exposure to methylmercury. Neurotoxicol Teratol. 1997; 19:417–428. [PubMed: 9392777]

Halladay AK, Wilson DT, Wagner GC, Reuhl KR. Trimethyltin-induced alterations in behavior are linked to changes in PSA-NCAM expression. Neurotoxicology. 2006; 27:137–146. [PubMed: 16426681]

Harada M. Congenital Minamata disease: intrauterine methylmercury poisoning. Teratology. 1978; 18:285–288. [PubMed: 362594]

Kempermann G, Jessberger S, Steiner B, Kronenberg G. Milestones of neuronal development in the adult hippocampus. Trends Neurosci. 2004; 27:447–452. [PubMed: 15271491]

Kuranaga E, Miura M. Nonapoptotic functions of caspases: caspases as regulatory molecules for immunity and cell-fate determination. Trends Cell Biol. 2007; 17:135–144. [PubMed: 17275304]

Lapham LW, Cernichiari E, Cox C, Myers GJ, Baggs RB, Brewer R, Shamlaye CF, Davidson PW, Clarkson TW. An analysis of autopsy brain tissue from infants prenatally exposed to methymercury. Neurotoxicology. 1995; 16:689–704. [PubMed: 8714873]

Leuner B, Gould E, Shors TJ. Is there a link between adult neurogensis and learning? Hippocampus. 2006; 16:216–224. [PubMed: 16421862]

Li CQ, Liu D, Huang L, Wang H, Zhang JY, Luo XG. Cytosine arabinoside treatment impairs the remote spatial memory function and induces dendritic retraction in the anterior cingulate cortex of rats. Brain Res Bull. 2008; 77:237–240. [PubMed: 18755251]

Lu TH, Hsieh SY, Yen CC, Wu HC, Chen KL, Hung DZ, Chen CH, Wu CC, Su YC, Chen YW, Liu SH, Huang CF. Involvement of oxidative stress-mediated ERK1/2 and p38 activation regulated mitochondria-dependent apoptotic signals in methylmercury-induced neuronal cell injury. Toxicol Lett. 2011; 204:71–80. [PubMed: 21549813]

Morris RGM, Garrund P, Rawlins JNP, O'Keefe J. Place navigation impaired in rats with hippocampal lesions. Nature. 1982; 297:681–683. [PubMed: 7088155]

Myers GJ, Davidson PW, Cox C, Shamlaye CF, Palumbo D, Cernichiari E, Sloane-Reeves J, Wilding GE, Kost J, Huang LS, Clarkson TW. Prenatal methylmercury exposure from ocean fish consumption in the Seychelles child development study. Lancet. 2003; 361:1686–1692. [PubMed: 12767734]

Newland MC, Paletz EM, Reed MN. Methylmercury and nutrition: adult effects of fetal exposure in experimental models. Neurotoxicology. 2008; 29:783–801. [PubMed: 18652843]

Newland MC, Reed MN, LeBlanc A, Donlin WD. Brain and blood mercury and selenium after chronic and developmental exposure to methylmercury. Neurotoxicology. 2006; 27:710–720. [PubMed: 16824603]

Newland MC, Reile PA. Blood and brain mercury levels after chronic gestational exposure to methylmercury in rats. Toxicol Sci. 1999; 50:106–116. [PubMed: 10445759]

Ogita K, Nishiyama N, Sugiyama C, Higuchi K, Yoneyama M, Yoneda Y. Regeneration of granule neurons after lesioning of hippocampal dentate gyrus: evaluation using adult mice treated with trimethyltin chloride as a model. J Neurosci Res. 2005; 82:609–621. [PubMed: 16273549]

Onishchenko N, Tamm C, Vahter M, Hokfelt T, Johnson JA, Johnson DA, Ceccatelli S. Developmental exposure to methylmercury alters learning and induces depression-like behavior in male mice. Toxicol Sci. 2007; 97:428–437. [PubMed: 17204583]

Rice D, Barone S Jr. Critical periods of vulnerability for the developing nervous system: evidence from humans and animal models. Environ Health Perspect. 2000; 108(Suppl 3):511–533. [PubMed: 10852851]

Rodier PM, Aschner M, Sager PR. Mitotic arrest in the developing CNS after prenatal exposure to methylmercury. Neurobehav Toxicol Teratol. 1984; 6:379–385. [PubMed: 6514102]

Rola R, Raber J, Rizk A, Otsuka S, VandenBerg SR, Morhardt DR, Fike JR. Radiation-induced impairment of hippocampal neurogenesis is associated with cognitive deficits in young mice. Experimental Neurology. 2004; 188:316–330. [PubMed: 15246832]

Schlessinger AR, Cowan WM, Gottlieb DI. An autoradiographic study of the time of origin and the pattern of granule cell migration in the dentate gyrus of the rat. J Comp Neurol. 1975; 159:149–175. [PubMed: 1112911]

Shirai K, Mizui T, Suzuki Y, Kobayashi Y, Nakano T, Shirao T. Differential effects of x-irradiation on immature and mature hippocampal neurons in vitro. Neurosci Lett. 2006; 399:57–60. [PubMed: 16483715]

Shors TJ, Townsend DA, Zhao M, Kozorovitskiy Y, Gould E. Neurogenesis may relate to some but not all types of hippocampal-dependent learning. Hippocampus. 2002; 12:578–584. [PubMed: 12440573]

Snyder JS, Hong NS, McDonald RJ, Wojtowicz JM. A role for adult neurogenesis in spatial long-term memory. Neuroscience. 2005; 130:843–852. [PubMed: 15652983]

Sokolowski K, Falluel-Morel A, Zhou X, Dicicco-Bloom E. Methylmercury (MeHg) elicits mitochondrial-dependent apoptosis in developing hippocampus and acts at low exposures. Neurotoxicology. 2011

Steiner B, Klempin F, Wang L, Kott M, Kettenmann H, Kempermann G. Type-2 cells as link between glial and neuronal lineage in adult hippocampal neurogenesis. Glia. 2006; 54:805–814. [PubMed: 16958090]

Stummann TC, Hareng L, Bremer S. Hazard assessment of methylmercury toxicity to neuronal induction in embryogenesis using human embryonic stem cells. Toxicology. 2009; 257:117–126. [PubMed: 19150642]

Suh H, Consiglio A, Ray J, Sawai T, D'Amour KA, Gage FH. In vivo fate analysis reveals the multipotent and self-renewal capacities of Sox2+ neural stem cells in the adult hippocampus. Cell Stem Cell. 2007; 1:515–528. [PubMed: 18371391]

Tamm C, Duckworth J, Hermanson O, Ceccatelli S. High susceptibility of neural stem cells to methylmercury toxicity: effects on cell survival and neuronal differentiation. J Neurochem. 2006; 97:69–78. [PubMed: 16524380]

Wagner JP, Black IB, DiCicco-Bloom E. Stimulation of Neonatal and Adult Brain Neurogenesis by Subcutaneous Injection of Basic Fibroblast Growth Factor. The Journal of Neuroscience. 1999; 19(14):6006–6016. [PubMed: 10407038]

Winocur G, Wojtowicz JM, Sekeres M, Snyder JS, Wang S. Inhibition of neurogenesis interferes with hippocampus-dependent memory function. Hippocampus. 2006; 16:296–304. [PubMed: 16411241]

Xu M, Yan C, Tian Y, Yuan X, Shen X. Effects of low level of methylmercury on proliferation of cortical progenitor cells. Brain Res. 2010; 1359:272–280. [PubMed: 20813099]

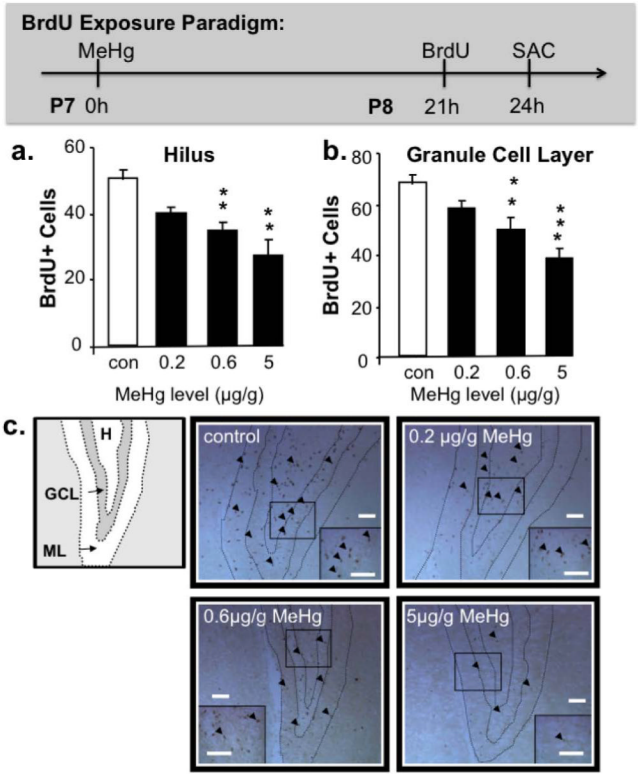

Figure 1. Effects of single MeHg exposures on BrdU+ cells in P7 hippocampus

There were significant decreases in S-phase labeled cells in both the (**a**) hilus and (**b**) granule cell layer of the dentate gyrus 24h after exposure to 0.6μg/g and 5μg/g MeHg. In (**c**), decreasing numbers of BrdU+ cells (arrowheads) can be observed in dentate gyrus sections with increasing exposures. (n=9 from 3 experiments; GCL: granule cell layer, H: hilus, ML: molecular layer **p<0.01, ***p<0.001; Scale bars = 100μm).

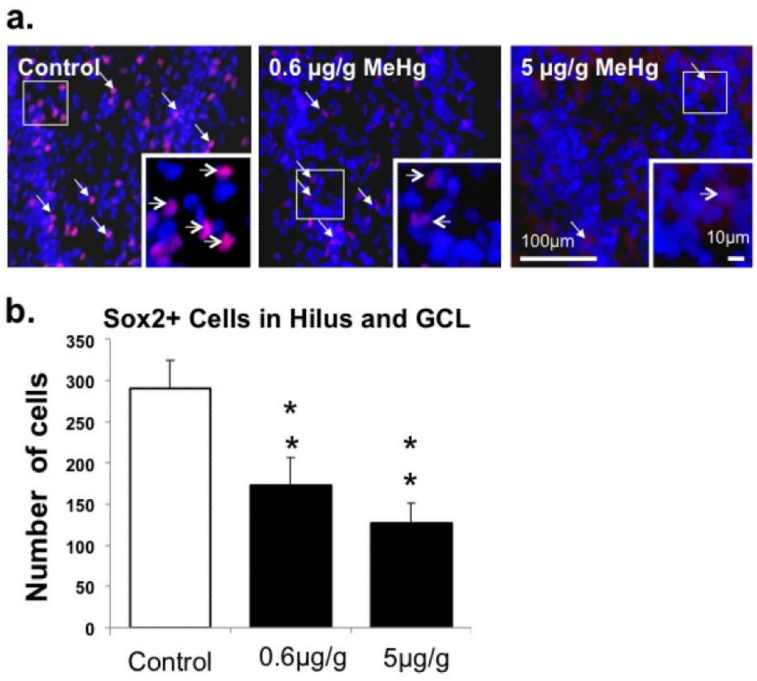

Figure 2. Effect of P7 MeHg exposure on Sox2+ cells in the hippocampus after 24h

(**a**) Sox2+ cells (red; arrows) and DAPI (blue) signals in the dentate gyrus. (**b**) Quantification of the number of Sox2+ cells in each exposure group. There were ≥ 2-fold decreases in Sox2-labeled cells after exposures to 0.6μg/g and 5μg/g MeHg. (n=9 from 3 experiments; **p<0.01).

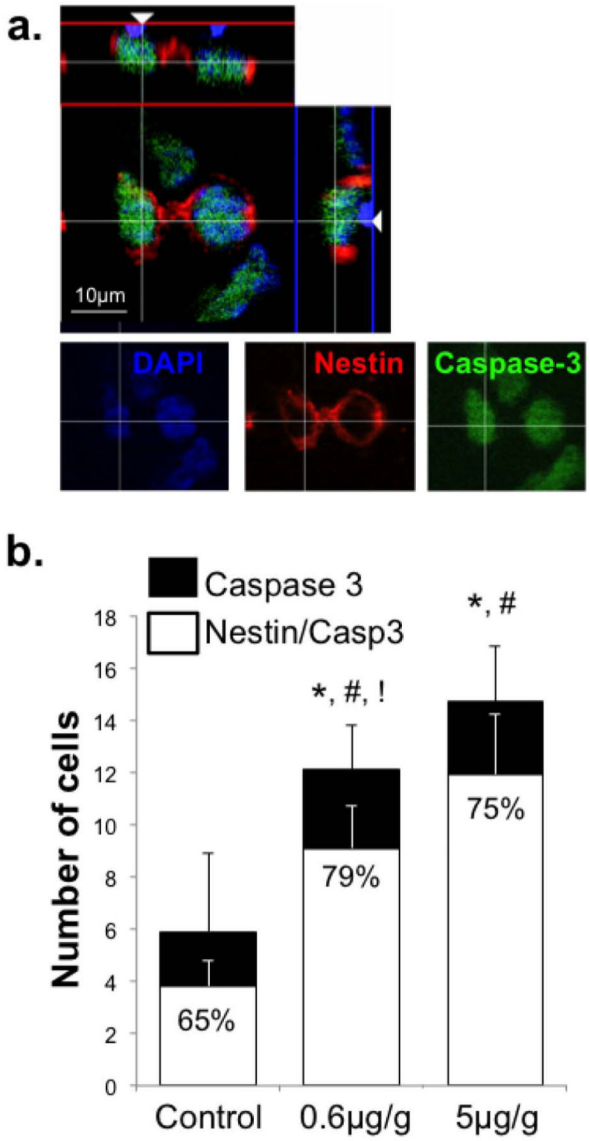

Figure 3. Acute MeHg exposure on P7 increases cleaved caspase-3+ cells and nestin-caspase-3 co-labeling in the hilus 24h later

(**a**) Cells triple-labeled for nestin (red), caspase-3 (green) and DAPI (blue). (**b**) The numbers of cleaved caspase-3+ as well as nestin+/caspase-3+ cells were quantified. There was an exposure-dependent increase in caspase-3 positive cells and double-labeled cells. The ratio of double-labeled nestin+/caspase-3+ cells to total caspase-3+ cells (presented as percent) increased after MeHg exposure indicating that the nestin-expressing precursors disproportionately contributed to the enhanced apoptotic population. (n=6 from 3 experiments; *compares total caspase-3+ cells ($p<0.0001$); #compares double-labeled cells (Nestin/Caspase-3);!compares the ratios expressed as a percent (Nestin/Caspase-3: Caspase-3); significance was defined as $p<0.05$).

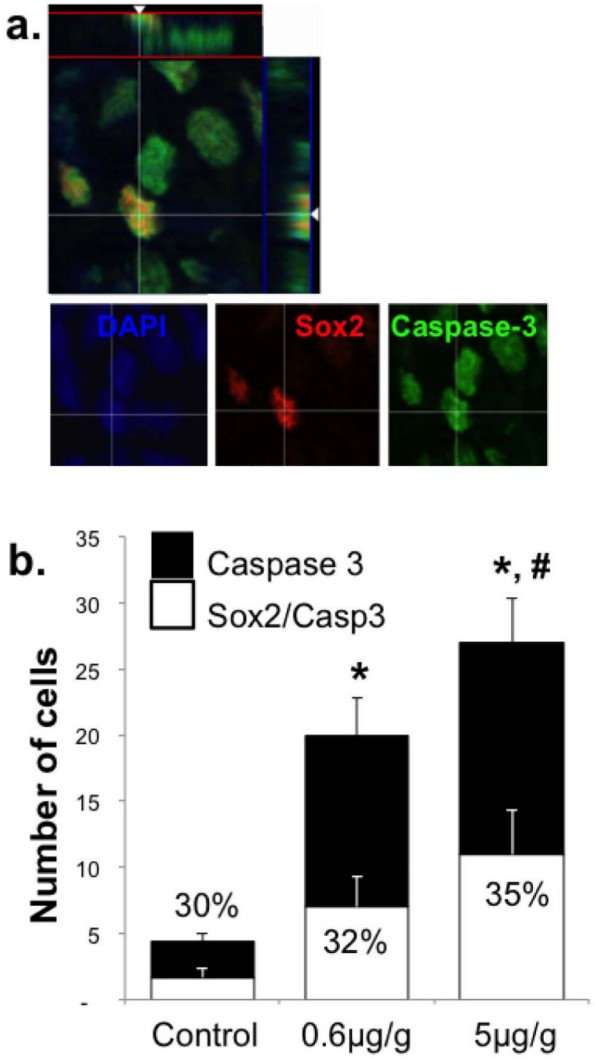

Figure 4. Acute MeHg exposure on P7 increases co-labeling of cleaved caspase-3 and Sox2 in the hilus 24h later

(**a**) Cells triple-labeled for Sox2 (red), caspase-3 (green) and DAPI (blue). (**b**) Quantification of cleaved caspase-3+ as well as Sox2+/caspase-3+ cells demonstrated an exposure-dependent increase in caspase-3 positive cells and double-labeled cells. There is no change in the ratio of double-labeled Sox2+/caspase-3+ cells to total caspase-3+ cells (presented as percent) after MeHg exposure. (n=6 from 3 experiments; *compares total caspase-3+ cells ($p<0.0001$); #compares double-labeled cells (Sox2/Caspase-3; $p<0.01$).

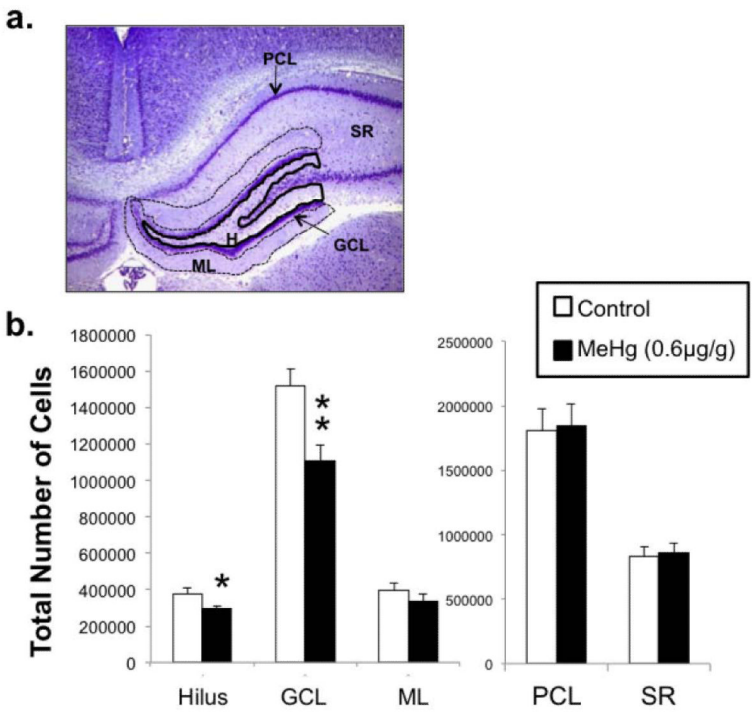

Figure 5. P21 cell number in the hippocampus after P7 exposure to 0.6μg/g MeHg

P7 rats were given a single sc injection of 0.6μg/g MeHg or PBS and unbiased stereology was performed on five regions of the P21 hippocampus as defined in (**a**) dentate gyrus hilus (H), granule cell layer (GCL), and molecular layer (ML) and the CA1-3 pyramidal cell layer (PCL) and stratum radiatum (SR). (**b**) Quantification of total cell numbers in each region. Low MeHg exposure elicited decreases in cell numbers in the H and GCL only, and not in ML, PCL or SR (n=9 from 3 experiments; *p<0.05, **p<0.01).

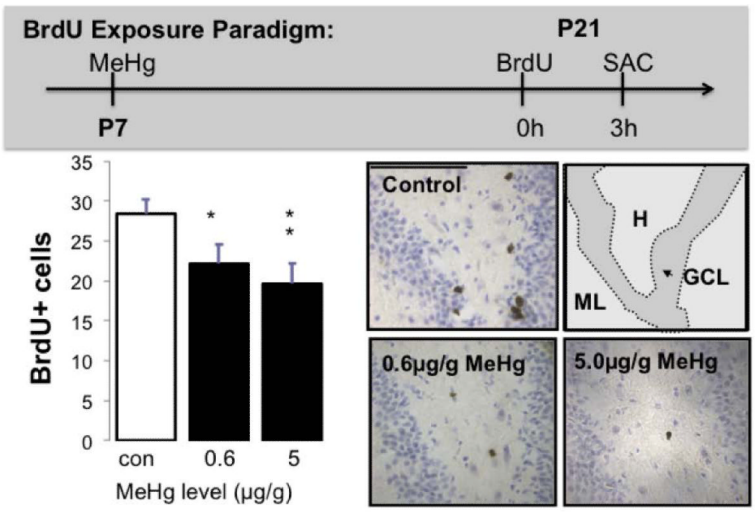

Figure 6. Effects of single P7 MeHg exposures on BrdU+ cells in P21 hilus

There were significant decreases in S-phase labeled cells in the P21 hilus of the dentate gyrus after exposure to 0.6μg/g and 5μg/g MeHg on P7. In (**b**), decreasing numbers of BrdU + cells (arrowheads) can be observed in dentate gyrus sections with increasing exposures. (n=12 from 4 experiments; *p<0.05, **p<0.01; Scale bars = 100μm).

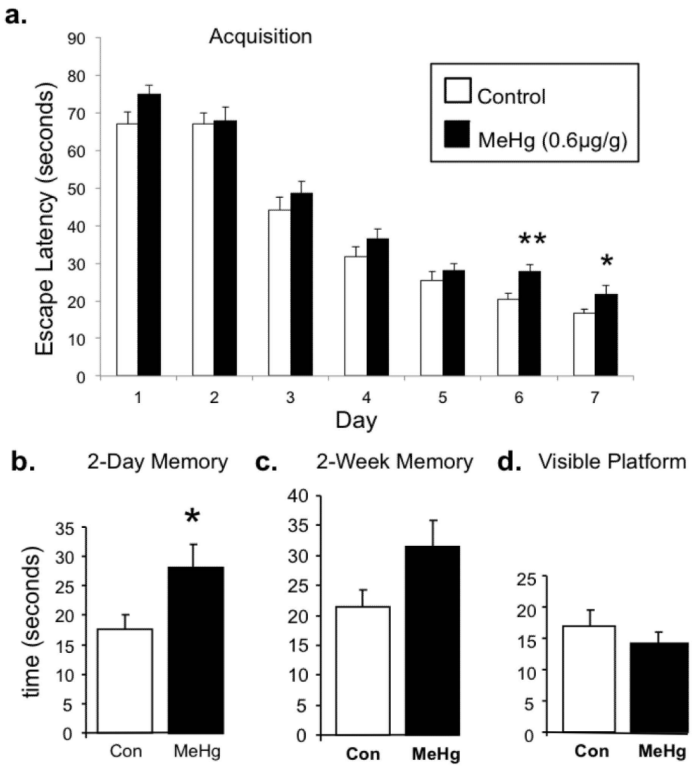

Figure 7. P35 learning and memory performance on Morris water maze after P7 exposure to 0.6µg/g MeHg

(**a**) The 7-day acquisition period shows learning in both groups, however, MeHg exposed animals had significantly longer escape latencies during the final two days of acquisition. (**b**) MeHg exposed animals also had longer escape latencies in the 2-day memory trial, (**c**) while there was a similar tendency in the 2-week memory trial (p=0.057). (**d**) There were no differences in the visible platform task. (n=30; *p<0.05, **p<0.01).

Table 1

Concentration of total Hg in hippocampus after P7 exposure

	P7 (2h)	P8 (24h)	P21 (2 weeks)	P35 (4 weeks)
0.6 μg/g MeHg	16 ± 38	383 ± 66*	2 ± 11	0 ± 38
5 μg/g MeHg	499 ± 24***	1963 ± 157***	310 ± 42*	0 ± 67

control 0±48